


RESEARCH ARTICLE | NOVEMBER 10 2003

Anisotropy of the magnetotransport in (Ga,Mn)As/MnAs paramagnetic-ferromagnetic hybrid structures

S. Ye; P. J. Klar; Th. Hartmann; W. Heimbrod; M. Lampalzer; S. Nau; T. Torunski; W. Stolz; T. Kurz; H.-A. Krug von Nidda; A. Loidl

 Check for updates

Appl. Phys. Lett. 83, 3927–3929 (2003)

<https://doi.org/10.1063/1.1625791>

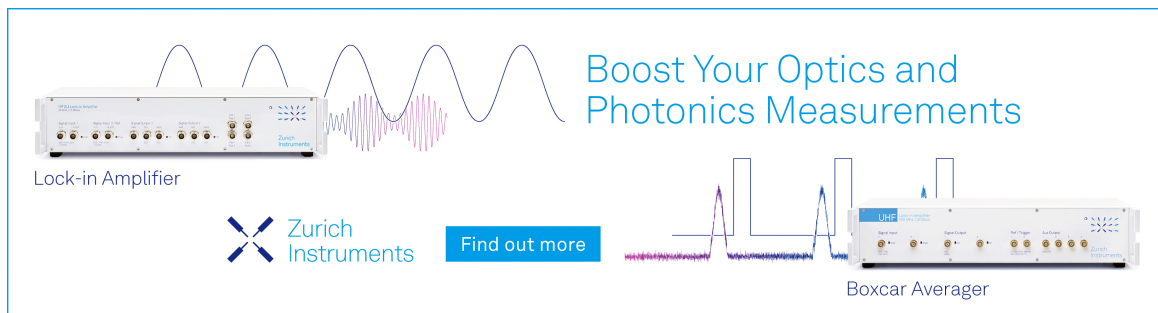


View Online




Export Citation

09 April 2024 09:00:52



Boost Your Optics and Photonics Measurements

Lock-in Amplifier

 Zurich Instruments

[Find out more](#)

Boxcar Averager

Anisotropy of the magnetotransport in (Ga,Mn)As/MnAs paramagnetic-ferromagnetic hybrid structures

S. Ye, P. J. Klar,^{a)} Th. Hartmann, W. Heimbrodt, M. Lampalzer, S. Nau, T. Torunski, and W. Stolz

Department of Physics and Material Sciences Center, Philipps-University, Renthof 5, 35032 Marburg, Germany

T. Kurz, H.-A. Krug von Nidda, and A. Loidl

Experimental Physics V and EKM, Institute of Physics, University of Augsburg, Universitätsstraße 2, 86135 Augsburg, Germany

(Received 17 June 2003; accepted 23 September 2003)

We investigated the temperature-dependent magnetoresistance of granular (Ga,Mn)As/MnAs hybrids grown on (100) GaAs in different transport geometries. The observed magnetoresistance effects are much bigger than for a corresponding (Ga,Mn)As reference sample without MnAs nanoclusters. We find that the magnetoresistance effects depend strongly on the chosen transport geometry. When the external field is perpendicular to the sample plane the effects are largest. The smallest effects occur when the external field is in the sample plane and parallel to the current. Furthermore, we have established by ferromagnetic resonance studies that the magnetic properties of the ensemble of ferromagnetic MnAs nanoclusters is similar for the magnetic field orientations studied. Therefore, the observed anisotropy of the magnetoresistance mainly reflects the difference in current path through the sample which leads to a variation of the degree of interaction between the free carriers in the matrix and nanoclusters. © 2003 American Institute of Physics.

[DOI: 10.1063/1.1625791]

Semiconductor-ferromagnetic hybrid structures are currently of interest as potential materials for spintronics and spin optoelectronics as they combine Curie temperatures T_C above room temperature and semiconductor properties.^{1,2} Possible hybrid structures are structures of alternating layers of ferromagnetic metals and paramagnetic semiconductors as well as structures where ferromagnetic nanoclusters are embedded in a paramagnetic semiconductor. An important aspect in the design of such structures for device applications is to maximize magnetoresistance (MR) effects. To date, there are only a few reports on the MR effects in granular semiconductor-ferromagnet hybrids such as $\text{Ga}_{1-x}\text{Mn}_x\text{As}/\text{MnAs}$,^{3,4} GaAs/ErAs ,⁵ GaAs/MnSb ,^{6,7} or $\text{Ge}_{1-y}\text{Mn}_y/\text{Mn}_{11}\text{Ge}_8$,⁸ where negative and positive MR effects are commonly observed.^{3,4,8} Here we study the temperature-dependent MR effect in the (Ga,Mn)As/MnAs hybrids for different transport geometries and its correlation to the magnetic properties of the MnAs clusters.

(Ga,Mn)As layers containing MnAs clusters of ellipsoidal shape were grown at 500°C by metalorganic vapor phase epitaxy on (100) GaAs substrates. The sample structure is depicted schematically in the inset of Fig. 1(a). The diameter of the clusters varies from about 35 to 120 nm and the corresponding height from 15 to 150 nm. The T_C of all hybrids is well above 300 K. For comparison we have grown a paramagnetic $\text{Ga}_{1-x}\text{Mn}_x\text{As}$ reference sample without MnAs clusters. The Mn content in the paramagnetic material was $x \approx 0.1\%$ for all samples. For the ferromagnetic resonance (FMR) measurements a standard X-band setup was

used.⁹ MR measurements were performed between 15 and 300 K and in magnetic fields (H) up to 10 T. H was applied either perpendicular (along GaAs [100]) or parallel (along [011]) to the sample plane. In the latter case, the magnetore-

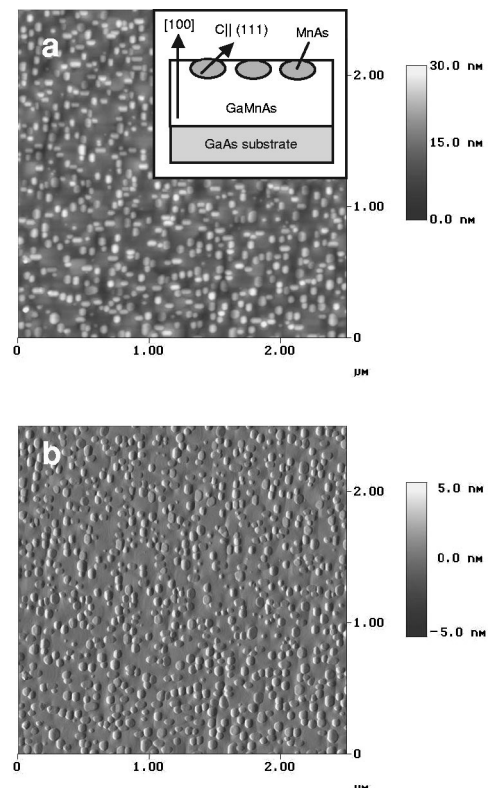


FIG. 1. (a) AFM height image of a (Ga,Mn)As/MnAs hybrid (b) corresponding amplitude image (i.e., height derivative profile). Inset: schematic sample structure.

^{a)}Author to whom correspondence should be addressed; electronic mail: klarp@mail.uni-marburg.de

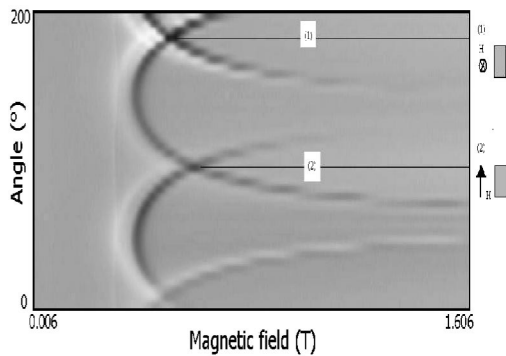


FIG. 2. Angular dependence of the FMR signal (field derivative of absorption in black and white scale) in the (Ga,Mn)As/MnAs hybrid. (1) The external magnetic field perpendicular to the sample surface along [100]. (2) the external magnetic field in the plane along [0-11]. $T = 150$ K.

sistance was measured with current I (along [011]) $\parallel H$ or I (along [0-11]) $\perp H$. The MR ratio is defined as $\Delta\rho(H)/\rho_0 = [\rho(H) - \rho_0]/\rho_0$, where ρ_0 and $\rho(H)$ are the resistivities in zero-field and at H , respectively. The structural properties of the MnAs nanoclusters in the (Ga,Mn)As matrix were studied by transmission electron microscopy as well as by atomic force microscopy (AFM).² Figure 1(a) shows exemplarily an AFM height image of the surface of the sample with the smallest clusters. The MnAs nanoclusters are embedded in the (Ga,Mn)As matrix close to the sample surface. They are distributed homogeneously and are all of comparable size. Figure 2 depicts the angular dependence of the FMR signal in the (Ga,Mn)As/MnAs hybrid with the smallest clusters. The axis of rotation (perpendicular to H) was chosen parallel to the GaAs [011] direction. The positions (1) and (2) in the figure correspond to field geometries where $H \parallel [100]$ and $H \parallel [0-11]$. Two distinct quasiparabolic resonance curves are observed assigned to subensembles of clusters of similar orientation. A detailed analysis of the FMR data reveals that the c axis of the hexagonal MnAs clusters is close to the four equivalent (111) directions of GaAs. The easy axis of magnetization of the MnAs clusters is always found in the basal plane perpendicular to the c axis.⁹ In particular, the behavior of the total magnetization of the MnAs clusters is comparable for the two field geometries. Furthermore, FMR and magnetization measurements reveal that there is also virtually no difference in the magnetization behavior for the two in-plane geometries where $H \parallel [011]$ and $H \parallel [0-11]$, respectively, for samples grown at 500 °C (in contrast to samples grown at 600 °C).²

Figure 3 depicts the temperature-dependence of the MR effect in the (Ga,Mn)As/MnAs hybrid with the smallest clusters for three different transport geometries. Figure 3(a) shows the temperature dependent MR in the geometry where H (along [100]) $\perp I$. At low temperatures, a strong negative MR is observed. At $T = 15$ K, the MR decreases slowly at low H , and then on further increasing H keeps decreasing at a constant rate without saturation. A MR of -30% is achieved at $H = 10$ T. With increasing temperature, the negative MR effect is suppressed and then changes to a positive MR at a temperature $T_1 = 40$ K. The magnitude of the positive MR effect increases further with increasing temperature and reaches a maximum at a temperature $T_2 = 60$ K. It always increases with increasing H and does not reach a satu-

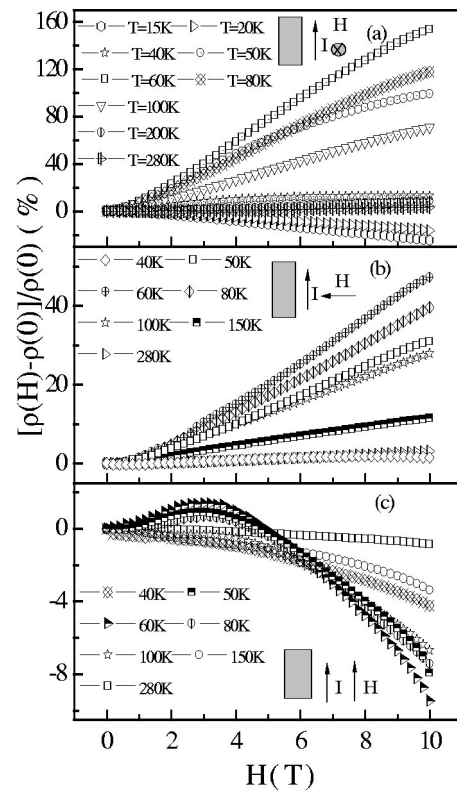


FIG. 3. Field-dependence of the magnetoresistance of a (Ga,Mn)As/MnAs hybrid at various temperatures for different transport geometries.

ration up to $H = 10$ T. For $H = 10$ T a MR value of 160% is observed at T_2 . Above T_2 , the MR effect becomes smaller again, but remains positive up to 300 K. Figure 3(b) shows the temperature dependence of the MR in the geometry where H (along [0-11]) $\perp I$. In this geometry, the MR behavior as a function of field and temperature is similar to that in the first geometry, but the magnitude of the effect is reduced. The maximum positive MR effect is only about 50% at $H = 10$ T and $T_2 = 60$ K. The MR effects in the (Ga,Mn)As/MnAs hybrids for the two geometries in Figs. 3(a) and 3(b) differ considerably in magnitude as well as field and temperature behavior from those observed for the $\text{Ga}_{1-x}\text{Mn}_x$ As samples ($x < 0.5\%$) without MnAs clusters.¹⁰ The MR effects in samples with clusters are more than an order of magnitude larger than in the reference samples without clusters. When H (along [0-11]) $\parallel I$, as depicted in Fig. 3(c), the MR effects are smallest. However, at low fields $H < 5$ T, the MR behavior is similar to that of the other two geometries. The MR changes very slowly with increasing H ; it changes from negative to positive with increasing temperature; and the MR effect is largest at $T_2 = 60$ K. However, at high fields $H > 5$ T the MR is always negative and keeps decreasing monotonically without saturation up to $H = 10$ T. The negative MR effect at 10 T is again largest at T_2 . However, the magnitude of MR effect in this orientation is comparable to that in the paramagnetic (Ga,Mn)As reference sample without MnAs nanoclusters.

Similar results for all three transport geometries were observed for samples with other cluster sizes. With increasing cluster size (i.e., diameter > 35 nm and height > 15 nm), both temperatures T_1 and T_2 were found to increase whereas the magnitude of the MR effect was found to decrease. Simi-

lar MR curves as a function of field and temperature were also measured on (Ga,Mn)As /MnAs hybrids prepared by other methods.^{3,4} Wellmann *et al.* reported a similar behavior for (Ga,Mn)As/MnAs hybrids with smaller clusters with diameters below 50 nm and observed the largest MR effects for the 50 nm clusters.³ This suggests that there exists an optimum cluster size where the MR effects are maximum. This is further corroborated by results of Akinaga *et al.* who found a similar temperature dependence of the MR effects, but much smaller than in this work, in (Ga,Mn)As/MnAs hybrids with cluster sizes below 10 nm.⁴ The temperature dependence of the MR effect appears to be an intrinsic feature of the (Ga,Mn)As/MnAs hybrid system, in particular, as the effect is almost independent of the preparation method. A similar temperature dependence was also observed in $\text{Ge}_{1-y}\text{Mn}_y:\text{Mn}_{11}\text{Ge}_8$ hybrids.⁸

Figure 4 summarizes the temperature dependence of the MR effects for the three transport geometries. In all three graphs the MR values at $H = 10$ T are depicted as a function of temperature for the (Ga,Mn)As/MnAs hybrid and for the (Ga,Mn)As reference sample without MnAs clusters. For all three geometries the magnitude of the MR effect is biggest at the characteristic temperature T_2 and approaches that of the sample without clusters at the highest temperatures. The MR effect due to the clusters is enhanced strongly in the (Ga,Mn)As/MnAs hybrid compared with the (Ga,Mn)As without MnAs clusters, when $I \perp H$ [Figs. 4(a) and (b)]. When $I \parallel H$, the MR effects are comparable in magnitude in both samples indicating that the effect of the clusters is weaker in this geometry [Fig. 4(c)]. On the other hand, we have established by ferromagnetic resonance studies and magnetization measurements that the magnetic properties of the ensemble of ferromagnetic MnAs nanoclusters is very similar for the three magnetic field orientations studied. Therefore, the observed anisotropy of the magneto-resistance for current direction $I \parallel H$ and $I \perp H$ mainly reflects the difference in current path through the sample. This leads to a variation of the degree of interaction between the free carriers in the paramagnetic matrix and the ferromagnetic MnAs nanoclusters. For $I \perp H$ the current path through the sample is extended due to the circular movement between two scattering events and the number of interactions between the free carriers and the ferromagnetic clusters is enhanced.

The MR effects in the (Ga,Mn)As/MnAs hybrids do not only depend on the microscopic interaction mechanism between the free carriers in the paramagnetic semiconductor host and the ferromagnetic MnAs clusters, but also depend strongly on the transport geometry and the resulting current path through the sample. The identification of the predominant microscopic scattering mechanisms leading to the observed MR effects requires further investigations. Other granular alloys where ferromagnetic clusters are embedded in a diamagnetic (metallic or insulating) matrix, at low volume fractions, always reveal large negative MR effects only.^{11–15} Large positive MR effects (referred to as extraordinary MR) always occur in high-mobility diamagnetic semiconductors with diamagnetic metal inclusions.^{16,17} The observation of positive as well as negative MR effects in

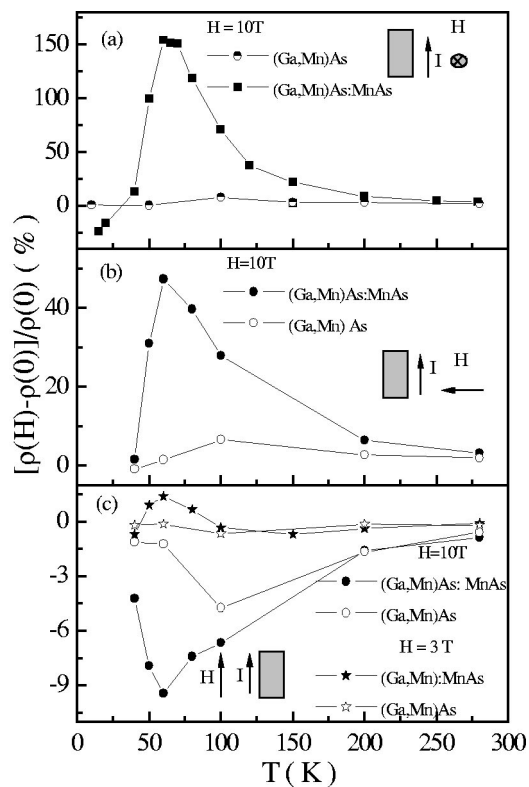


FIG. 4. Temperature dependence of the magnetoresistance value at $H = 10$ T for the (Ga,Mn)As:MnAs hybrid and a (Ga,Mn)As reference sample without MnAs clusters.

paramagnetic-ferromagnetic granular hybrids^{3–8} suggests that the paramagnetism of the matrix plays a major role in the microscopic processes determining the MR effects.

- ¹M. Tanaka, *Semicond. Sci. Technol.* **17**, 327 (2002).
- ²M. Lampalzer, K. Volz, W. Treutmann, S. Nau, T. Torunski, K. Megges, J. Lorberth, and W. Stolz, *J. Cryst. Growth* **248**, 474 (2003).
- ³P. J. Wellmann, J. M. Garcia, J. L. Feng, and P. M. Petroff, *Appl. Phys. Lett.* **73**, 3291 (1998).
- ⁴H. Akinaga, J. De Boeck, G. Borghs, S. Miyayoshi, A. Asamitsu, W. Van Roy, Y. Tomioka, and L. H. Kuo, *Appl. Phys. Lett.* **72**, 3368 (1998).
- ⁵D. R. Schmidt, A. G. Petukhov, M. Foygel, J. P. Ibbetson, and S. J. Allen, *Phys. Rev. B* **82**, 823 (1999).
- ⁶M. Mizuguchi, H. Akinaga, K. Ono, and M. Oshima, *J. Appl. Phys.* **87**, 5639 (2000).
- ⁷H. Akinaga, M. Mizuguchi, K. Ono, and M. Oshima, *Appl. Phys. Lett.* **76**, 2600 (2000).
- ⁸Y. D. Park, A. Wilson, A. T. Hanbicki, J. E. Mattson, T. Ambrose, G. Spanos, and B. T. Jonker, *Appl. Phys. Lett.* **78**, 2739 (2001).
- ⁹Th. Hartmann, M. Lampalzer, P. J. Klar, W. Stolz, W. Heimbrodt, H.-A. Krug von Nidda, A. Loidl, and L. Svistov, *Physica E (Amsterdam)* **13**, 572 (2002).
- ¹⁰S. Ye, P. J. Klar, T. Henning, M. Lampalzer, W. Stolz, and W. Heimbrodt, *J. Supercond.* **16**, 423 (2003).
- ¹¹S. Zhang and P. M. Levy, *J. Appl. Phys.* **73**, 5315 (1993).
- ¹²J. Q. Wang and G. Xiao, *Phys. Rev. B* **49**, 3982 (1994).
- ¹³F. Badia, X. Battle, A. Labarta, M. L. Watson, A. B. Johnston, and J. N. Chapman, *J. Appl. Phys.* **82**, 677 (1997).
- ¹⁴A. Milner, A. Gerber, B. Groisman, M. Karpovsky, and A. Gladkikh, *Phys. Rev. Lett.* **76**, 475 (1996).
- ¹⁵D. K. Petrov, L. Krusin-Elbaum, J. Z. Sun, C. Feild, and P. R. Duncombe, *Appl. Phys. Lett.* **75**, 995 (1999).
- ¹⁶S. A. Solin, T. Thio, D. R. Hines, and J. J. Heremans, *Science* **289**, 1530 (2000).
- ¹⁷J. Moussa, L. R. Ram-Mohan, J. Sullivan, T. Zhou, D. R. Hines, and S. A. Solin, *Phys. Rev. B* **64**, 184410 (2000).